Model-independent test for *CPT* violation using long-baseline and atmospheric neutrino experiments

Daljeet Kaur*

SGTB Khalsa College, University of Delhi, Delhi 110007, India

(Received 21 October 2019; accepted 16 February 2020; published 12 March 2020)

Charge-parity-time (*CPT*) symmetry governs that the oscillation parameters for neutrinos and antineutrinos are to be identical. Different mass and mixing parameters for these particles may give us a possible hint for *CPT* violation in the neutrino sector. Using this approach, we discuss the ability of long-baseline and atmospheric neutrino experiments to determine the difference between mass squared splittings ($\Delta m^2_{32} - \Delta \bar{m}^2_{32}$) and atmospheric mixing angles ($\sin^2\theta_{23} - \sin^2\bar{\theta}_{23}$) of neutrinos and antineutrinos. We show the joint sensitivity of the T2K, NOvA, and INO experiments to such *CPT* violating observables in different possible combinations of octant for neutrinos and antineutrinos.

DOI: 10.1103/PhysRevD.101.055017

I. INTRODUCTION

The fact that neutrinos have mass and flavor mixed are strongly confirmed with the discovery of neutrino oscillations [1–5]. The existence of neutrino masses is in fact the first solid experimental fact requiring physics beyond the Standard Model. Under the assumption of conservation of the fundamental *CPT* symmetry, both neutrino and antineutrino oscillations are described by three mass eigenstates ν_1, ν_2, ν_3 with mass values m_1, m_2, and m_3 that are connected to the flavor states ν_e, ν_μ, and ν_τ by a mixing matrix U [6,7]. The neutrino or antineutrino oscillation probability depends on three mixing angles, θ_{12}, θ_{23}, θ_{13}; two independent mass differences, $|\Delta m^2_{32}|$, Δm^2_{21}; where $\Delta m^2_{32} = m^2_3 - m^2_2$ and $\Delta m^2_{21} = m^2_2 - m^2_1$; and a *CP* violating phase δ_{CP}. The primary goals of present and future neutrino oscillation experiments are to perform precision measurements of the neutrino parameters, determine the right order of neutrino masses (i.e., the sign of Δm^2_{32}), determine the right octant [lower octant (LO) if $\theta_{23} < 45°$ and higher octant (HO) if $\theta_{23} > 45°$] and to determine the value of *CP* phase δ_{CP}.

With the increasing knowledge of the standard neutrino oscillation parameters, searches for the symmetry-breaking effects become also possible. For example, with the nonzero value of θ_{13} [8,9], it became possible to search for *CP*-violation in the neutrino sector via the differences in the oscillation probabilities of neutrinos and antineutrinos. Similarly, *CPT* violation has been studied by several neutrino oscillation experiments under various assumptions [10–30]. According to the conservation of *CPT* symmetry, the mass-squared splitting and mixing angles are expected to be identical for neutrinos and antineutrinos. Therefore, an independent measurement of neutrino and antineutrino oscillation parameters and their comparison can be treated as a model independent way to test the *CPT*-conservation or it could possibly give us a sign for *CPT*-violation[31–37].

In this paper, we use the model independent way to test the *CPT* theorem under the standard three neutrino paradigm. We consider the possibility that the oscillation probability governed by neutrino mass splitting or mixing angle is different as compared to that of antineutrinos. Thus, the differences between neutrino and antineutrino oscillation parameters might be regarded as *CPT* violating observables. We perform realistic simulations for the current and future long-baseline oscillation experiments (T2K, NOvA) and atmospheric neutrino experiment (ICAL-INO). We explore the potential of these experiments to test the *CPT* conservation and the *CPT* violation, assuming nonidentical neutrino and antineutrino oscillation parameters. Since, the octant of neutrinos or antineutrinos is still unknown, we also show the potential of these experiments in different possible combinations of octants for neutrinos and antineutrinos.

This paper is organized as follows. A brief introduction of the experiments used in the analysis is given in Sec. II. In Sec. III, we describe the details of simulations work for atmospheric (INO) and long-baseline experiments (T2K and NOvA) separately. In Sec. IV, we show the experimental sensitivity of T2K, NOvA and INO experiments considering *CPT* is conserved [Subsection IV B] followed by the *CPT* violation sensitivities [Subsection IV C]. We explore the joint sensitivity for these experiments under Subsection IV D. Finally, we conclude our results in Sec. V.

*daljeet.kaur97@gmail.com

II. EXPERIMENTAL SPECIFICATIONS

(i) The INO-ICAL experiment: The India-based Neutrino Observatory (INO)[38] is an atmospheric neutrino experiment, which will be located at Bodi West hills in the Theni district of South India. A 50 kton magnetized ICAL detector will be the main detector at INO to address the current issues of neutrino physics like neutrino mass hierarchy, octant of θ_{23} and the precise determination of neutrino mixing parameters. The 1 km rock overburden above the site will act as a natural shield from the background of cosmic rays. The ICAL detector will be of rectangular shape of dimensions $48m \times 16m \times 14.5m$ having three modules. Each module weighing about 17 kton with the dimensions $16m \times 16m \times 14.5m$. Each module will consist of 151 layers of 5.6 cm thick iron plates with alternate gaps of 4 cm where the active detector element will be placed. In the first phase of INO, glass resistive plate chambers (RPCs) will be used as active detector to track the charged particles produced through the interaction of muon neutrinos with iron target. Another important feature of the INO-ICAL experiment is the application of a magnetic field of 1.5 T that will help in distinguishing the charge of the interacting particles. This distinction is crucial for the precise determination of relative ordering of neutrino mass states (neutrino mass hierarchy) and other parameters. The INO-ICAL experiment is sensitive to atmospheric muons only. Hence, it will observe interactions of muon type neutrinos. The ICAL experiment will also measure the energy of hadron shower to improve the energy reconstruction of events, and hence the overall sensitivity to neutrino parameters [40,41].

(ii) The NOvA experiment: The NOvA (NuMi off-axis ν_e appearance) [42,43] is a long-baseline neutrino experiment that uses an NuMI beam source at Fermilab. It is designed to study the $\nu_\mu \to \nu_e$ appearance oscillations and $\nu_\mu \to \nu_\mu$ survival oscillations. It uses a high intensity proton beam with a beam power of 0.7 MW. It consists of two detectors; near detector (ND) and far detector (FD), which are functionally identical and 14.6 mrad off axis from the Fermilab NuMI beam to receive a narrow-band neutrino energy spectrum near 2 GeV. The ND is 1 km away from the beam source to detect the unoscillated beam and a 14-kton liquid scintillator FD is located in Ash River, Minnesota, with a baseline of 810 km from the Fermilab to detect the oscillated neutrino beam. The long-baseline of NOvA enhances the matter effect and allows probing of the neutrino mass ordering. The experiment is designed to operate in neutrino mode (using neutrino beam flux) and antineutrino mode (using antineutrino beam flux). The long base-line oscillation channels used in NOvA includes 1. ν_e appearance, 2. ν_μ disappearance, 3. NC disappearance. NOvA has the potential to measure the precise value of neutrino mixing angles, determine neutrino mass hierarchy and can investigate the CP violation in the lepton sector. It is scheduled to run 5 years in ν mode followed by 5 years in $\bar{\nu}$ mode.

(iii) The T2K experiment: The T2K (Tokai to Kamioka) [44,45] experiment is a long-baseline neutrino oscillation experiment. The experiment uses an intense proton beam of 0.77 MW power generated by the J-PARC accelerator in Tokai, Japan. T2K composed of a neutrino beamline, a near detector complex (ND280), and a far detector (Super-Kamiokande) located 295 km away from J-PARC. T2K is an off-axis experiment which generate the narrow-band neutrino beam using proton synchrotron at J-PARC. The off-axis angle is set at 2.5 degree so that the narrow-band ν_μ beam peaks at energy of 2 GeV, which maximizes the effect of the neutrino oscillation at 295 km and minimizes the background to electron neutrino appearance detection. The near detector site at nearly 280 m from the production target and houses on-axis and off-axis detectors. The on-axis detector (INGRID), composed of an array of iron/scintillator sandwiches, measures the neutrino beam direction and profile. The off-axis detector is composed of a water-scintillator detector, the tracker consisting of time projection chambers (TPCs) and fine grained detectors (FGDs) optimized to study charged current interactions; and an electromagnetic calorimeter (ECal). The whole off-axis detector is placed in a 0.2 T magnetic field. The far detector, Super-Kamiokande, is located at Kamioka Mine, Japan. The detector cavity lies under the peak of a mountain, with 1000 m of rock overburden. It has a 22.5 kt water Cherenkov detector consisting of a welded stainless steel tank, 39 m in diameter and 42 m tall. The detector contains approximately 13,000 photomultiplier tubes (PMTs) that image neutrino interactions in pure water. The main goal of T2K experiment is to measure the last unknown lepton sector mixing angle θ_{13} by observing ν_e appearance in a ν_μ beam. It also aims to make a precision measurement of the known oscillation parameters, $|\Delta m^2_{32}|$ and θ_{23}, via ν_μ disappearance studies. Other goals of the experiment include various neutrino cross-section measurements and sterile neutrino searches.

III. ANALYSIS METHODOLOGY

(i) For atmospheric neutrino experiment: The magnetized ICAL detector enables separation of neutrino and antineutrino interactions for atmospheric events, allowing an independent measurement of the ν_μ and

$\bar{\nu}_\mu$ oscillation parameters. We analyze the reach of the iron calorimeter for ν_μ and $\bar{\nu}_\mu$ oscillations separately using a three flavor analysis including the Earth matter effects. A large number of unoscillated NUANCE [46] neutrino events have been generated using HONDA [47] atmospheric neutrino fluxes for an exposure of 50 kt × 1000 years of the ICAL detector. Analysis has been performed by normalizing these events to 500 kt-yr exposure for the ICAL detector. Each charged-current (CC) neutrino event is characterized by its energy and zenith angle. Oscillation effects have been introduced via a Monte-Carlo reweighting algorithm as described in earlier works [41,48,49].

Each oscillated neutrino or antineutrino event is divided as a function of twenty muon energy bins (E_μ), twenty muon zenith angle ($\cos\theta_\mu$) and five hadron energy bins (E_{hadron}) of optimized bin width as mentioned in Ref. [50]. These binned data are then folded with detector efficiencies and resolution functions as provided by the INO collaboration [51,52] for the reconstruction of neutrino and antineutrino events separately. We use a "pulled" χ^2 [53] method based on Poisson probability distribution to compare the expected and observed data. The functions $\chi^2(\nu_\mu)$ and $\chi^2(\bar{\nu}_\mu)$ are calculated separately for the independent measurement of neutrino and antineutrino oscillation parameters. The two χ^2 can be added to get the combined $\chi^2(\nu_\mu + \bar{\nu}_\mu)$ as

$$\chi^2(\nu_\mu + \bar{\nu}_\mu) = \chi^2(\nu_\mu) + \chi^2(\bar{\nu}_\mu). \tag{1}$$

The ν and $\bar{\nu}$ events are separately binned into direction and energy bins. For different energy and direction bins, the χ^2 function is minimized with respect to these four parameters along with the nuisance parameters to take the systematic uncertainties into account as considered in earlier ICAL analyses [41,48]. Other simulation inputs are summarized as shown in Table I.

(ii) For long-baseline neutrino experiments: The beamline experiments are suitable for both neutrino and antineutrino mode, it is easy to study the sensitivity for the oscillation parameters for neutrino and antineutrino independently. In order to quantify the sensitivities of the long-baseline experiments T2K and NOvA experimental setups, we use GLoBES [54,55] as a simulator. For the NovA experiment simulations, we use 3 years ν and 3 years $\bar{\nu}$ running mode with beam power of 0.7 MW with 20e20 POT/year. The NOvA detector properties considered in this analysis are taken as in Ref. [56]. We have considered input files for T2K from the general long baseline experiment simulator (GLoBES) package [54,55] and the updated experimental description of T2K are taken from [57,58]. In this analysis, we have used 5 years ν and 5 years $\bar{\nu}$ running modes for T2K with beam power of 0.75 MW. We analyze the neutrino events from ν_e appearance and ν_μ disappearance oscillation channels and antineutrino events from $\bar{\nu_e}$ appearance and $\bar{\nu_\mu}$ disappearance oscillation channels. For parameter-estimation, we make use of a chi-squared statistics that is a function of independent physics parameters for neutrinos and antineutrinos. For a given set of neutrino and antineutrino oscillation parameters, we compute the expected number of signal and background events as a function of energy for the experiment of interest. The values of χ^2 are evaluated for ν and $\bar{\nu}$ separately using the standard rules as described in GLoBES. Other detailed description of simulation inputs are shown in Table II.

TABLE I. Experimental specifications used in the analysis for INO atmospheric neutrino experiment.

Characteristics	INO
Source	Atmospheric Neutrinos
Run time	10 years for ν_μ and $\bar{\nu}_\mu$
Detector	50 kton Iron Calorimeter
Charge identification efficiency	∼99% for μ^- and μ^+ for few GeV muons as given in Ref. [51]
Direction reconstruction efficiency	∼1° for few GeV muons as in Ref. [51]
Systematics	20% flux normalization, 10% cross section, 5% tilt error, 5% zenith angle error and 5% overall systematics error as in Refs. [41,48]

IV. ANALYSIS

A. Neutrino and antineutrino oscillation parameters

Here, we introduce the notation used to describe neutrino and antineutrino oscillations used in the analysis. We use the neutrino oscillation parameters as three mixing angles, θ_{12}, θ_{23}, θ_{13}; two independent mass differences, Δm^2_{32}, Δm^2_{21}, and a CP phase δ_{CP}. Similarly, antineutrino parameters are described with a bar over them as three mixing angles, $\bar{\theta}_{12}$, $\bar{\theta}_{23}$, $\bar{\theta}_{13}$; two independent mass differences, $\Delta\bar{m}^2_{32}$, $\Delta\bar{m}^2_{21}$, and a CP phase $\bar{\delta}_{CP}$. The analysis considers only normal mass ordering, therefore only positive values of Δm^2_{32} or $\Delta\bar{m}^2_{32}$ have been used. For discussing differences between neutrino and antineutrino oscillation parameters, we use notation $\Delta(x) = x - \bar{x}$; where x is any oscillation parameters. So, $\Delta x = 0$ corresponds to identical oscillation parameters for ν and $\bar{\nu}$ or CPT conserved assumption and $\Delta x \neq 0$ corresponds to the CPT violation assumption. Since all the experiments considered in this paper are quite sensitive to atmospheric oscillation parameters, we mainly discuss the experimental sensitivities for finding out the difference

TABLE II. Experimental specifications used in the analysis for long-baseline experiments.

Characteristics	NOvA	T2K
Baseline	810 km	295 km
Run time	3 year ν and 3 year $\bar{\nu}$	5 year ν and 5 year $\bar{\nu}$
Detector	14 kton	22.5 kton
signal efficiency	26% for ν_e and 41% $\bar{\nu_e}$ signal 100% for both ν_μ CC and $\bar{\nu_\mu}$ CC	87% for both ν_e and $\bar{\nu_e}$ signal 100% for both ν_μ CC and $\bar{\nu}_\mu$ CC
Background efficiency	0.83% ν_μ CC, 0.22% $\bar{\nu_\mu}$ CC 2% ν_μ NC, 3% $\bar{\nu_\mu}$ NC 26%(18%) ν_e and $\bar{\nu_e}$ beam contamination	considered as given in Refs. [57,58]
Systematics	5% signal normalization error 10% background normalization error	2% signal normalization error 20% background normalization error

between the atmospheric mass squared splittings i.e., $\Delta(\Delta m^2_{32}) = \Delta m^2_{32} - \Delta\bar{m}^2_{32}$ and mixing angle difference i.e., $\Delta(\sin^2\theta_{23}) = \sin^2\theta_{23} - \sin^2\bar{\theta}_{23}$.

The global best fit values of oscillation parameters which are kept fixed through out the analysis are given as: $\sin^2\theta_{13}(\bar{\theta}_{13}) = 0.0234$, $\sin^2\theta_{12}(\bar{\theta}_{12}) = 0.313$, $\Delta m^2_{12}(\Delta\bar{m}^2_{12}) = 7.6\times10^{-5}$ eV^2. Since, the ICAL is insensitive to the variation of δ_{CP} phase [59], hence it is kept fixed at 0°. However, NOvA and T2K are sensitive to δ_{CP} so we marginalized the δ_{CP} in range 0–360° for the predicted data set. To find the sensitivities for atmospheric mass-squared splittings and mixing angles, oscillation parameters (Δm^2_{32}, $\Delta\bar{m}^2_{32}$, $\sin^2\theta_{23}$, and $\sin^2\bar{\theta}_{23}$) are allowed to fit in the range given in Table III.

B. Test for the *CPT* symmetry

In this section, we discuss the capabilities of NOvA, T2K and INO experiments to test the *CPT*-theorem. We show how well the neutrino and antineutrino can be measured independently from one another assuming *CPT* is a good symmetry. We consider the oscillation parameters for ν and $\bar{\nu}$ are identical and show the allowed regions for the parameters of interest assuming *CPT* is conserved. This identical parameters ($\nu - \bar{\nu} = 0$) is then taken as null hypothesis for analysis presented in Sec. IV C.

We test the sensitivities for ν oscillation parameters ($\Delta m^2_{32}, \sin^2\theta_{23}$) and $\bar{\nu}$ oscillation parameters ($\Delta\bar{m}^2_{32}$, $\sin^2\bar{\theta}_{23}$). In order to do so we proceed as follows. First, a fake dataset is generated at the fixed true values of ν or $\bar{\nu}$ oscillation parameters and then a two dimensional grid search is performed for the predicted dataset in the allowed ranges of the parameters as mentioned in Table III. Further, χ^2 is calculated between the fake dataset and predicted dataset for each set of true values of oscillation parameters. The functions $\chi^2(\nu)$ and $\chi^2(\bar{\nu})$ are calculated separately as an independent measurement of ν and $\bar{\nu}$. A joint result from the combined neutrino and antineutrino analysis is also shown. The two χ^2 can be added to get the combined analysis results $\chi^2(\nu+\bar{\nu})$ as mentioned in Eq. (1).

TABLE III. The neutrino and antineutrino oscillation parameters and their range.

Oscillation parameters	allowed fit range
Δm^2_{32} (eV^2)	$(2.0\text{–}3.0)\times10^{-3}$
$\Delta\bar{m}^2_{32}$ (eV^2)	$(2.0\text{–}3.0)\times10^{-3}$
$\sin^2\theta_{23}$	0.3–0.7
$\sin^2\bar{\theta}_{23}$	0.3–0.7

The results of the neutrino, antineutrino, and their joint data analyses have been shown on a single frame projecting over two-dimensional regions with allowed regions at 90% confidence level (CL) in the atmospheric plane [$\Delta m^2_{32}(\bar{m^2}_{32}), \sin^2\theta_{23}(\bar{\theta}_{23})$].

Figures 1–3 show the expected sensitivities obtained from NOvA, T2K, and INO experiments respectively having best fit values as $\sin^2\theta_{23}(\bar{\theta}_{23}) = 0.4$ [lower octant (LO)], 0.5 [maximal mixing (MM)], and 0.6 [higher octant (HO)] with $\Delta m^2_{32}(\Delta\bar{m}^2_{32}) = 2.45\times10^{-3}$ eV^2.

Results are shown for LO, MM, and for HO as left, middle, and right plots, respectively. It can be observed from these sample plots that for all the mentioned experiments, there is a clear difference between neutrino's and antineutrino's parameters space when they are analyzed independently. Neutrino only analysis give more stringent or precise parameter's space comparable to antineutrino only analysis. However, the $\nu+\bar{\nu}$ joint results are found to be more precise as compared to independent ν and $\bar{\nu}$ analyses. An overall comparison of the precision for the measurement of $(\Delta m^2_{32}, \sin^2\theta_{23})$ obtained from these experiments at the maximal mixing is shown in Table IV. We would like to mention that precision measurement of these parameters is not the main focus of this paper but it is interesting that assuming *CPT* is conserved, there is a difference between the independent measurement of neutrino and antineutrino oscillation parameters as shown in Table IV. This motivates us to do the *CPT* violation test where we can use this study as our null hypothesis.

The octant of ν and $\bar{\nu}$ plays an important role in the neutrino and antineutrino parameter estimation. One can

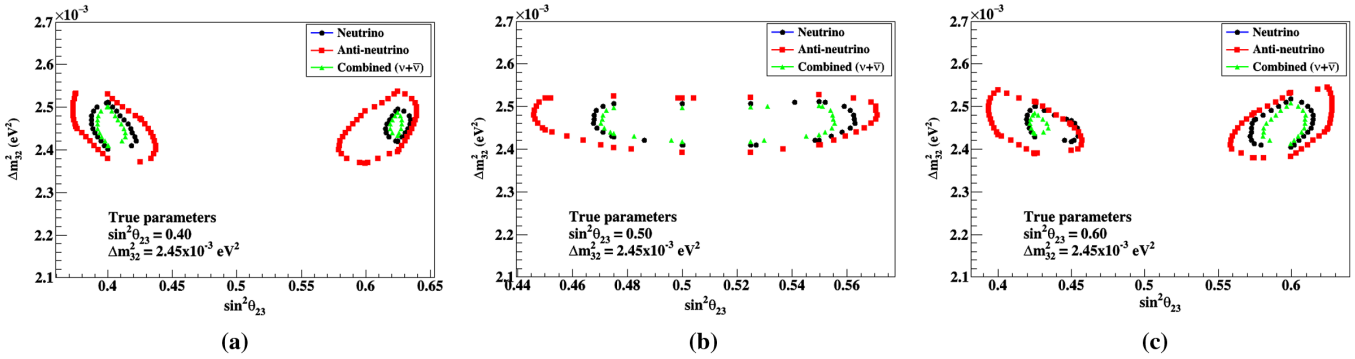

FIG. 1. 90% C.L. expected region obtained from NOvA experiment for lower octant ($\sin^2\theta_{23} = 0.40$)[Left], maximal mixing ($\sin^2\theta_{23} = 0.50$)[Middle], and for higher octant ($\sin^2\theta_{23} = 0.60$)[Right] with $\Delta m^2_{32} = 2.45 \times 10^{-3}$ eV^2, assuming *CPT* is conserved. Red, black, and green contours are obtained as a results of antineutrino, neutrino, and combined ($\nu + \bar{\nu}$) analysis, respectively.

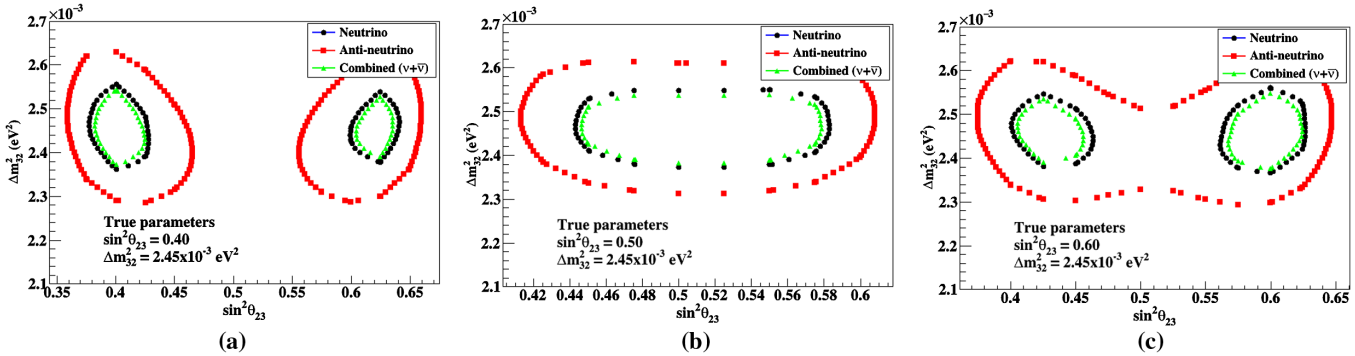

FIG. 2. 90% C.L. expected region obtained from T2K experiment for lower octant ($\sin^2\theta_{23} = 0.40$)[Left], maximal mixing ($\sin^2\theta_{23} = 0.50$)[Middle], and for higher octant ($\sin^2\theta_{23} = 0.60$)[Right] with $\Delta m^2_{32} = 2.45 \times 10^{-3}$ eV^2, assuming *CPT* is conserved. Red, black, and green contours are obtained as a results of antineutrino, neutrino, and combined ($\nu + \bar{\nu}$) analysis, respectively.

observe a clear octant degeneracy from Figs. 1 and 2. The NOvA experiment clearly shows two degenerate solutions of $\sin^2\theta_{23}$ at the lower octant as well as higher octant [Figs. 1(a) and 1(c)] in all the analyses [neutrino, antineutrino, and combined ($\nu + \bar{\nu}$)]. However, T2K experiment shows a clear octant degeneracy at the LO in all the analyses [Fig. 2(a)], while at the higher octant side, two degenerate solutions exist only in antineutrino and combined ($\nu + \bar{\nu}$) analyses [Fig. 2(c)]. Figure 3 depicts that INO does not show any octant degeneracy in the mixing angle.

C. Test for the *CPT* violation

We study the NOvA, T2K, and INO experiment's sensitivity to measure *CPT* violation by determining how well these experiments can rule out the conserved *CPT* assumption for neutrino and antineutrino parameters.

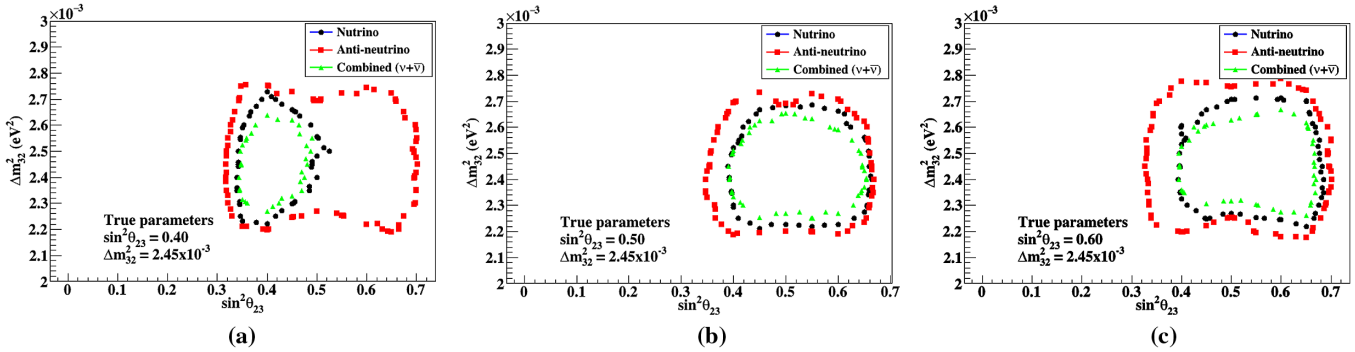

FIG. 3. 90% C.L. expected region obtained from INO experiment for lower octant ($\sin^2\theta_{23} = 0.40$)[Left], maximal mixing ($\sin^2\theta_{23} = 0.50$)[Middle], and for higher octant ($\sin^2\theta_{23} = 0.60$)[Right] with $\Delta m^2_{32} = 2.45 \times 10^{-3}$ eV^2, assuming *CPT* is conserved. Red, black, and green contours are obtained as a results of antineutrino, neutrino, and combined ($\nu + \bar{\nu}$) analysis, respectively.

TABLE IV. Precision measurement of parameters $\Delta m^2_{32}(\Delta\bar{m}^2_{32})$ and $\sin^2\theta_{23}(\bar{\theta}_{23})$ for NOvA, T2K and INO experiment for maximal mixing $\sin^2\theta_{23}(\bar{\theta}_{23}) = 0.5$ and $\Delta m^2_{32}(\Delta\bar{m}^2_{32}) = 2.45 \times 10^{-3}$ eV^2.

Analysis Mode	$\Delta m^2_{32}(or\Delta\bar{m}^2_{32})$ in %			$\sin^2\theta_{23}(or\bar{\theta}_{23})$ in %		
Experiments	NOvA	T2K	INO	NOvA	T2K	INO
Antineutrinos	2.43	6.15	11.02	11.50	19.00	30.61
Neutrinos	1.95	3.61	9.11	8.83	13.65	25.97
Combined $(\nu + \bar{\nu})$	1.56	3.19	7.80	7.97	12.90	25.26

For this, we started with the assumption that neutrino and antineutrinos have different mass-squared splittings and mixing angles such that the difference $[\Delta(\Delta m^2_{32}) = (\Delta m^2_{32} - \Delta\bar{m}^2_{32}) \neq 0]$, and $[\Delta\sin^2\theta_{23} = (\sin^2\theta_{23} - \sin^2\bar{\theta}_{23}) \neq 0]$. To rule out the null hypothesis, i.e., identical oscillation parameters for neutrinos and antineutrinos, a fake dataset is generated at a given set of true values of neutrino and antineutrino oscillation parameters (Δm^2_{32}, $\sin^2\theta_{23}$, $\Delta\bar{m}^2_{32}$, $\sin^2\bar{\theta}_{23}$). A four dimensional grid search is performed for the predicted dataset. χ^2 is calculated between the fake dataset and predicted dataset for each set of true values of oscillation parameters. Now, the true values of the oscillation parameters are not fixed at single value rather it also varied in the range as mentioned in Table III and same procedure is repeated again for each set of true values. We calculated $\Delta(\Delta m^2_{32})$ and $\Delta\sin^2\theta_{23}$. To find out the sensitivity for the difference $\Delta(\Delta m^2_{32})$, a minimum χ^2 has been binned as a function of difference in the true values of $\Delta(\Delta m^2_{32})$ keeping marginalization over $\Delta\sin^2\theta_{23}$ and for the sensitivity for difference of mixing angles $\Delta\sin^2\theta_{23}$, same has been done with the marginalization over $\Delta(\Delta m^2_{32})$. Further, for each set of difference $\Delta(\Delta m^2_{32})$ or $\Delta\sin^2\theta_{23}$, we calculate $\Delta\chi^2 = \chi^2 - \chi^2_{\min}$ and plot it as the functions of set of differences.

It is quite possible that in nature neutrino and antineutrino may lie in same or different octant. We also try to simulate the data considering this possibility to obtained the detector sensitivity for $\Delta(\Delta m^2_{32})$ and $\Delta\sin^2\theta_{23}$ in combination of different octants. There are four possible combinations of octants for neutrino and antineutrinos:

Case 1: νs and $\bar{\nu}$s both in higher octant (HO) [$\sin^2\theta_{23}(\sin^2\bar{\theta}_{23})$ in range 0.5–0.7]

Case 2: νs and $\bar{\nu}$s both in lower octant (LO) [$\sin^2\theta_{23}(\sin^2\bar{\theta}_{23})$ in range 0.3–0.5]

Case 3: νs in HO and $\bar{\nu}$s in LO

Case 4: νs in LO and $\bar{\nu}$s in HO

Figures 4–6 show the one dimensional experimental sensitivities of $\Delta(\Delta m^2_{32})$ and $\Delta\sin^2\theta_{23}$ for the NOvA, T2K, and INO experiments, respectively.

Figure 4 [Left] shows the NOvA sensitivity for the mass squared splitting difference parameter $\Delta(\Delta m^2_{32})$ for all possible cases of octants for ν and $\bar{\nu}$ as mentioned earlier. It has been observed that for case 3 and case 4 (where ν and $\bar{\nu}$ are assumed to be in different octant) gives slightly better sensitivity for $\Delta(\Delta m^2_{32})$ than the similar octant combinations (case 1 and case 2). NOvA can rule out the CPT conserved scenario by measuring $\Delta(\Delta m^2_{32})$ with 2σ significance level $\sim 0.15 \times 10^{-3}$ eV^2 for the similar octant combinations (case 1 and case 2) and it is $\sim 0.10 \times 10^{-3}$ eV^2 for different octant combination (case 3 and case 4).

The right panel of Fig. 4 shows the NOvA sensitivity for $\Delta\sin^2\theta_{23}$. It is found that the NOvA is most sensitive for $\Delta\sin^2\theta_{23}$ only if the neutrinos and antineutrinos are in the same octant (either LO or HO) and out of this, case 2, where ν and $\bar{\nu}$ both in lower octant (LO) gives the slightly better sensitivity ($>3\sigma$ when $|\Delta\sin^2\theta_{23}| = 0.08$]) than case 1 where ν and $\bar{\nu}$ both in higher octant (HO). But, if neutrino and antineutrino octants are different, the sensitivity is almost $<2\sigma$ in the range $[-0.4, 0]$ of $\Delta\sin^2\theta_{23}$ for octant case 3 [ν in HO and $\bar{\nu}$ in LO] and it is $<3\sigma$ in the range [0, 0.4)] of $\Delta\sin^2\theta_{23}$ for octant case 4 [ν in LO and $\bar{\nu}$ in

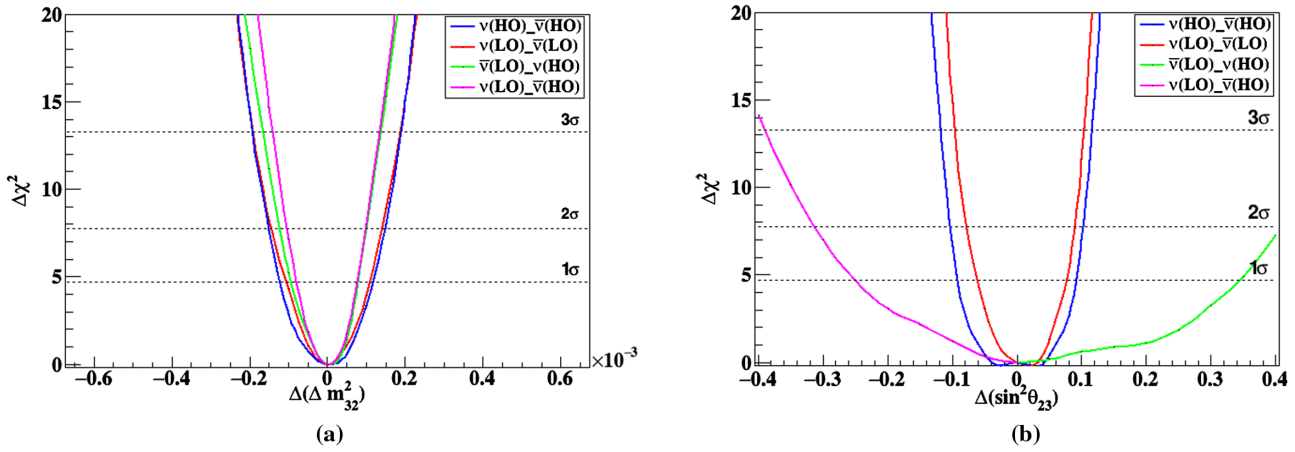

FIG. 4. NOvA experiment sensitivity for $\Delta(\Delta m^2_{32})$ eV^2 [Left] and $\Delta\sin^2\theta_{23}$ [Right] for different possible combinations of octant for ν and $\bar{\nu}$ having nonidentical oscillation parameters.

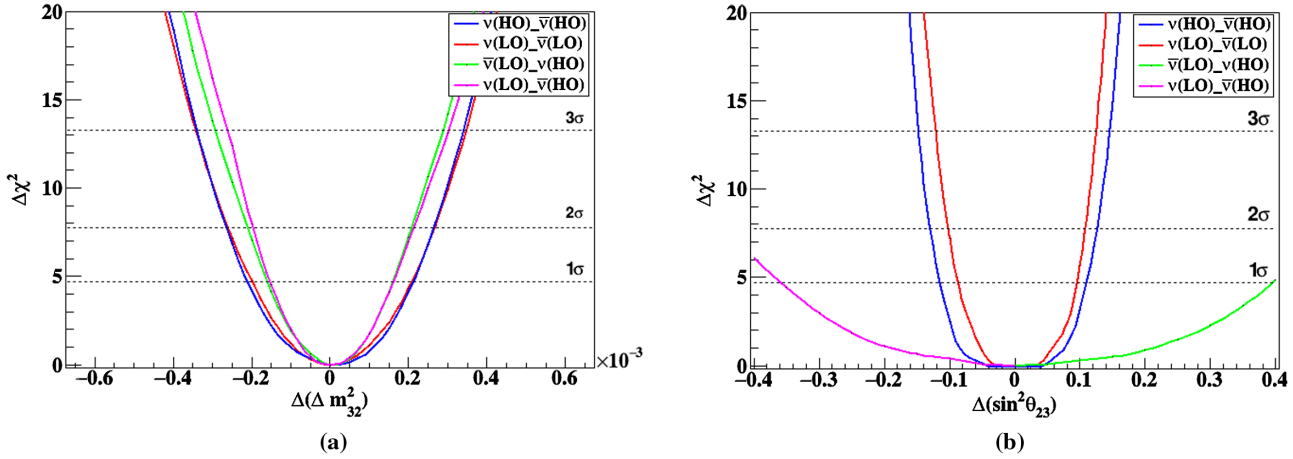

FIG. 5. The T2K experiment sensitivity for $\Delta(\Delta m^2_{32})$ eV^2 [Left] and $\Delta \sin^2\theta_{23}$ [Right] for different possible combinations of octant for ν and $\bar{\nu}$ having nonidentical oscillation parameters.

HO]. So we can say that for the NOvA experiment, similar octants for ν and $\bar{\nu}$ are favorable.

Figure 5 shows the sensitivities to $\Delta(\Delta m^2_{32})$ and $\Delta \sin^2\theta_{23}$ for the T2K experiment. The left panel of Fig. 5 depicts the T2K sensitivity to rule out the *CPT* conserved scenario [$\Delta(\Delta m^2_{32})$] for all possible combinations of octants assumed for neutrinos and antineutrinos. We observed that for T2K, opposite octant combination (case 3 and case4) for ν and $\bar{\nu}$ gives slightly better sensitivity than the similar octant combinations (case 1 and case 2). T2K can rule out the *CPT* conserved scenario by measuring $\Delta(\Delta m^2)$ as 0.2×10^{-3} eV^2 with 2σ significance level for the similar octant combinations (case 1 and case 2) and it is $\sim 0.275 \times 10^{-3}$ eV^2 for different octant combination (case 3 and case 4).

The right panel of Fig. 5 shows that T2K sensitivity for the difference of mixing angles $\Delta \sin^2\theta_{23}$. Similar to the NOvA experiment, the T2K experiment is also found to be most sensitive for the ($\Delta \sin^2\theta_{23}$) only if νs and $\bar{\nu}$s are in same octant (either LO or HO) and case 2 gives the better results than case 1. If different octant assumed for neutrino and antineutrinos [case 3 and case 4], T2K sensitivity for $\Delta \sin^2\theta_{23}$ is almost $< 1\sigma$ in the given range. So we can say that similar to the NOvA experiment, case 1 and case 2 are also most favorable for T2K experiment.

Similarly, Fig. 6 shows the sensitivities to $\Delta(\Delta m^2_{32})$ and $\Delta \sin^2\theta_{23}$ for the atmospheric INO-ICAL experiment. It is clear for the left panel of the Fig. 6 that ICAL detector can rule out the null hypothesis of identical mass-squared splittings for neutrino and antineutrinos with 2σ significance level for almost all possible combinations of octants if the $|\Delta(\Delta m^2_{32})|$ is roughly around 0.5×10^{-3} eV^2. And, similar to the NOvA and T2K experiment, it is also found to be least sensitive for the difference of neutrino and antineutrino mixing angles ($\Delta \sin^2\theta_{23}$) for the octant case 3 and 4 [Figure 6(b)]. For similar octant combinations for neutrino and antineutrino, the sensitivity of the ICAL detector is almost similar to the NOvA and T2K experiments and can rule out the identical mixing angles for neutrino and antineutrino with 2σ significance level if the $|\Delta \sin^2\theta_{23}| = 0.08$.

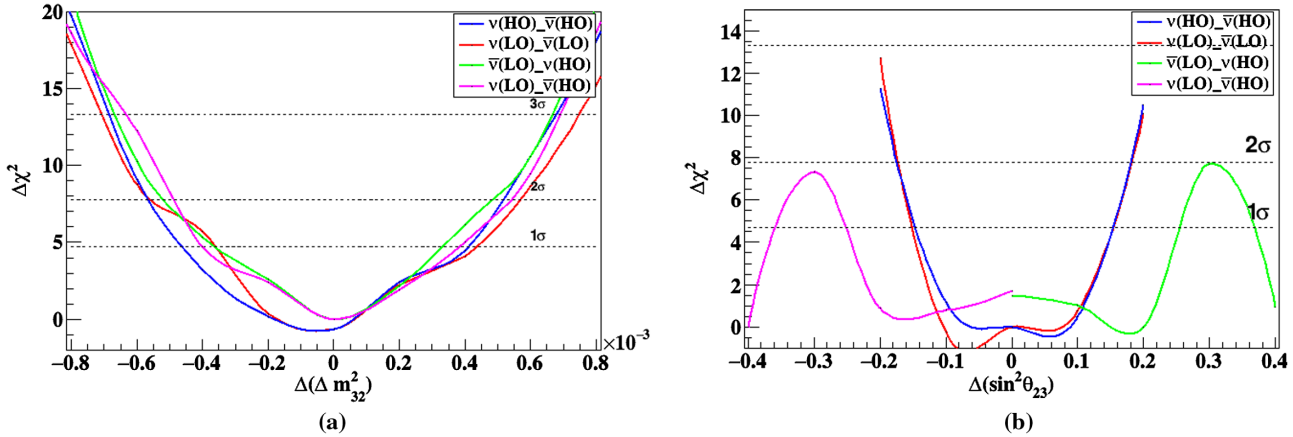

FIG. 6. The INO experiment sensitivity for $\Delta(\Delta m^2_{32})$ eV^2 [Left] and $\Delta \sin^2\theta_{23}$ [Right] for different possible combinations of octant for ν and $\bar{\nu}$ having nonidentical oscillation parameters.

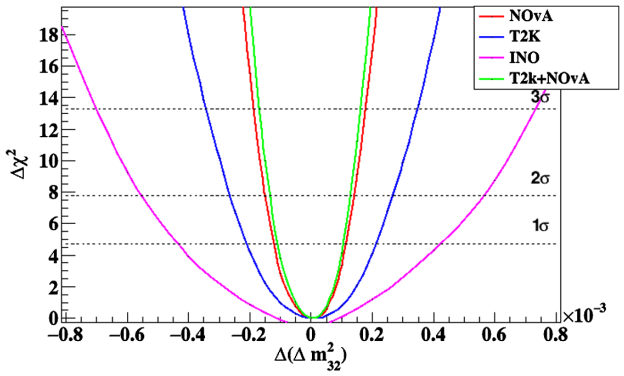

FIG. 7. Experimental sensitivity of the NOvA, T2K, and the INO experiments for $\Delta(\Delta m^2_{32})$ eV^2.

D. Combined experimental sensitivities for $\Delta(\Delta m^2_{32})$ and $\Delta \sin^2\theta_{23}$

As it is clear from Sec. IV C, with the considered exposure and run time, the NOvA and T2K experiments' sensitivity is quite better compared to the INO-ICAL experimental sensitivity. Hence, we also show a combined long baseline (T2K and NOvA) sensitivity for a better estimation of $\Delta(\Delta m^2_{32})$ and $\Delta \sin^2\theta_{23}$. We observed that $\Delta(\Delta m^2_{32})$ is not affected from different octant considerations for neutrinos and antineutrinos. So, we show an overall estimation for the measurement of $\Delta(\Delta m^2_{32})$ [Fig. 7] from the NOvA, T2K, and INO-ICAL experiments.

A quantitative comparison of potential of these experiments for $\Delta(\Delta m^2_{32})$ is shown in Table V. It is clear from Fig. 7 and Table V that the NOvA sensitivity is almost comparable to joint (NOvA + T2K) sensitivity for $\Delta(\Delta m^2_{32})$. We expect that NOvA experiment itself can able to rule out the identical oscillation parameters (*CPT* is conserved) by measuring $\Delta(\Delta m^2_{32})$ in comparison to NOvA + T2K combined analyses. Similarly, Fig. 8 shows the combined sensitivity of the NOvA, T2K and INO experiments for the measurement of $\Delta \sin^2\theta_{23}$ in different possible combination of octant as mentioned in Sec. IV C. Here, we find that although NOvA experiment is good enough to constrain $\Delta \sin^2\theta_{23}$ for case 1 and case 2, but on combining T2K and NOvA data, the sensitivity for $\Delta \sin^2\theta_{23}$ significantly increases for octant case 3 and case 4, where neutrinos and antineutrinos are assumed to be in

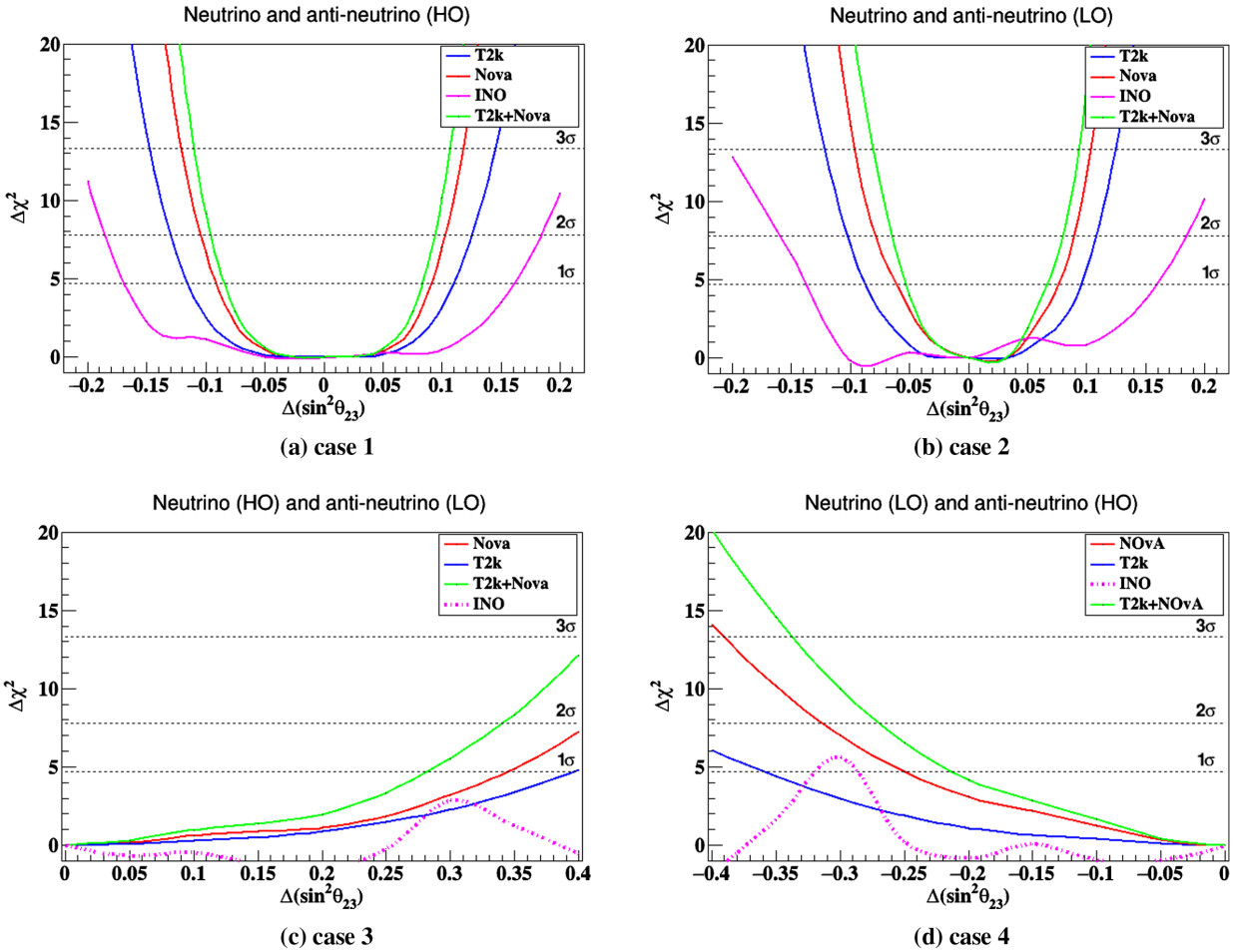

FIG. 8. Combined sensitivity of the NOvA, T2K, and INO experiments for $\Delta \sin^2\theta_{23} = \sin^2\theta_{23} - \sin^2\bar{\theta}_{23}$ when (a) ν and $\bar{\nu}$ in HO, (b) ν and $\bar{\nu}$ in LO, (c) ν in HO and $\bar{\nu}$ in LO and (d) when ν in LO and $\bar{\nu}$ in HO.

TABLE V. $|\Delta(\Delta m^2_{32})|$ and $|\Delta \sin^2\theta_{23}|$ sensitivity at the 1σ confidence level.

$\|\Delta(\Delta m^2_{32})\| \times 10^{-3}$ eV^2				
Osc.parameter	NOvA	T2K	INO	T2K + NOvA
$\|\Delta(\Delta m^2_{32})\|$	0.10	0.22	0.40	0.10
		$\|\Delta \sin^2\theta_{23}\|$		
Octant Case 1	0.1	0.13	0.16	0.07
Octant Case 2	0.08	0.12	0.17	0.09
Octant Case 3	0.34	0.4	$<1\sigma$	0.28
Octant Case 4	0.24	0.36	$<1\sigma$	0.21

different octant. A quantitative comparison of the sensitivity for $\Delta \sin^2\theta_{23}$ in different octants is shown in Table V.

V. SUMMARY AND CONCLUSIONS

In this paper we have performed a comprehensive comparative analysis for the *CPT* violation sensitivities using long-baseline (NOvA and T2K) and atmospheric neutrino (the INO-ICAL) experiments. First, we explored how well neutrino and antineutrino oscillation parameters are independently constrained by these experiments. Further, we estimated the potential of these experiments to test the hypothesis that neutrino and antineutrino oscillation parameters are identical, as governed by the *CPT* theorem. We presented a detailed discussion on the sensitivities for the *CPT* violation observables ($\Delta(\Delta m^2_{32})$ and $\Delta \sin^2\theta_{23}$) assuming four possible cases of octants for neutrinos and antineutrinos. We show that the experiments (NOvA, T2K, and INO-ICAL) are able to constrain these observables for all possible combinations of octants. Individually each experiment is able to measure $\Delta(\Delta m^2_{32})$ quite significantly irrespective of different octant combinations, but the measurement of $\Delta \sin^2\theta_{23}$ is largely affected by the existence of neutrinos and antineutrinos in a particular octant. We observed that all considered experiments are giving precise determination of $\Delta \sin^2\theta_{23}$ if both neutrinos and antineutrinos are assumed to have similar octant combinations (either LO or HO) and these experiments are least sensitive for different octant combinations for neutrinos and antineutrinos. So, we can say that similar octant combination (either LO or HO) for ν and $\bar{\nu}$ is a favorable condition for precise determination of $\Delta \sin^2\theta_{23}$ for all considered experiments. One can get a better sensitivity for the estimation of $\Delta(\Delta m^2_{32})$ and $\Delta \sin^2\theta_{23}$ significantly if we combine the results from different experiments. We study the joint sensitivity of both the long-baseline experiments (T2K + NOvA). Our study shows that with the proposed fiducial volume and run time, the NOvA detector independently found the best among all the considered experiments for constraining these parameters as shown in Table V. NOvA sensitivity is almost comparable to joint (NOvA + T2K) sensitivity for $\Delta(\Delta m^2_{32})$. However, NOvA + T2K joint results enhances the sensitivities for $\Delta \sin^2\theta_{23}$ if the neutrinos and antineutrinos are in different octants. The present *CPT* bounds at 1σ confidence interval are summarized in Table V.

ACKNOWLEDGMENTS

The author would like to thank University of Delhi R&D grants for providing the support for this research. Author would also like to thank Dr. Sanjeev Kumar, Dr. Md. Naimuddin, Prof. Brajesh Chandra Choudhary and Prabhjot Singh for many fruitful discussions related to this work.

[1] Q. R. Ahmad *et al.* (SNO Collaboration), Phys. Rev. Lett. **89**, 011301 (2002).
[2] Y. Fukuda *et al.* (Super-Kamiokande Collaboration), Phys. Rev. Lett. **81**, 1562 (1998).
[3] Y. Fukuda *et al.* (Super-Kamiokande Collaboration), Phys. Rev. Lett. **82**, 2644 (1999).
[4] S. H. Ahn *et al.* (K2K Collaboration), Phys. Lett. B **511**, 178 (2001).
[5] K. Eguchi *et al.* (KamLAND Collaboration), Phys. Rev. Lett. **90**, 021802 (2003).
[6] B. Pontecorvo, Zh. Eksp. Teor. Fiz. **33**, 549 (1957) [Sov. Phys. JETP **6**, 429 (1958)].
[7] B. Pontecorvo, Zh. Eksp. Teor. Fiz. **53**, 1717 (1968) [Sov. Phys. JETP **26**, 984 (1968)].
[8] J. Ahn *et al.* (RENO Collaboration), Phys. Rev. Lett. **108**, 191802 (2012).
[9] F. An *et al.* (DAYA-BAY Collaboration), Phys. Rev. Lett. **108**, 171803 (2012).
[10] D. Colladay and V. A. Kostelecky, Phys. Rev. D **55**, 6760 (1997).
[11] A. de Gouvêa, Phys. Rev. D **66**, 076005 (2002).
[12] G. Barenboim, L. Borissov, J. Lykken, and A. Y. Smirnov, J. High Energy Phys. 10 (2002) 001.
[13] G. Barenboim, L. Borissov, and J. Lykken, Phys. Lett. B **534**, 106 (2002).
[14] G. Barenboim, J. F. Beacom, L. Borissov, and B. Kayser, Phys. Lett. B **537**, 227 (2002).
[15] J. N. Bahcall, V. Barger, and D. Marfatia, Phys. Lett. B **534**, 120 (2002).
[16] G. Barenboim, and J. Lykken, Phys. Lett. B **554**, 73 (2003).
[17] A. Datta, R. Gandhi, P. Mehta, and S. Uma Sankar, Phys. Lett. B **597**, 356 (2004).

[18] V. A. Kostelecky and M. Mewes, Phys. Rev. D **70**, 031902 (2004).
[19] V. A. Kostelecky and M. Mewes, Phys. Rev. D **69**, 016005 (2004).
[20] H. Minakata and S. Uchinami, Phys. Rev. D **72**, 105007 (2005).
[21] A. de Gouvêa and Y. Grossman, Phys. Rev. D **74**, 093008 (2006).
[22] J. S. Diaz, V. A. Kostelecky, and M. Mewes, Phys. Rev. D **80**, 076007 (2009).
[23] J. S. Diaz and A. Kostelecky, Phys. Rev. D **85**, 016013 (2012).
[24] A. Kostelecky and M. Mewes, Phys. Rev. D **85**, 096005 (2012).
[25] J. S. Díaz, T. Katori, J. Spitz, and J. M. Conrad, Phys. Lett. B **727**, 412 (2013).
[26] A. Chatterjee, R. Gandhi, and J. Singh, J. High Energy Phys. 06 (2014) 045.
[27] T. Ohlsson and S. Zhou, Nucl. Phys. **B893**, 482 (2015).
[28] K. Abe *et al.* (Super-Kamiokande Collaboration), Phys. Rev. D **91**, 052003 (2015).
[29] C. A. Argüelles, T. Katori, and J. Salvado, Phys. Rev. Lett. **115**, 161303 (2015).
[30] J. S. Diaz and T. Schwetz, Phys. Rev. D **93**, 093004 (2016).
[31] G. Barenboim and J. D. Lykken, Phys. Rev. D **80**, 113008 (2009).
[32] P. Adamson *et al.* (MINOS Collaboration), Phys. Rev. Lett. **110**, 251801 (2013).
[33] K. Abe *et al.* (T2K Collaboration), Phys. Rev. D **96**, 011102 (2017).
[34] K. Abe *et al.* (Super-Kamiokande Collaboration), Phys. Rev. Lett. **107**, 241801 (2011).
[35] T. Ohlsson and S. Zhou, Nucl. Phys. **B893**, 482 (2015).
[36] A. de Gouvêa, and K. J. Kelly, Phys. Rev. D **96**, 095018 (2017).
[37] Z. A. Dar, D. Kaur, S. Kumar, and M. Naimuddin, J. Phys. G **46**, 065001 (2019).
[38] ICAL Collaboration, Pramana J. Phys, **88**, 79 (2017).
[39] D. Kaur, A. Kumar, A. Gaur, P. Kumar, M. Hasbuddin, S. Mishra, P. Kumar, and M. Naimuddin, Nucl. Instrum. Methods Phys. Res., Sect. A **774**, 74 (2015).
[40] A. Ghosha and S. Choubey, J. High Energy Phys. 10 (2013) 174.
[41] D. Kaur, M. Naimuddin, and S. Kumar, Eur. Phys. J. C **75**, 156 (2015).
[42] R. B. Patterson, Nucl. Phys. B, Proc. Suppl. **235–236**, 151 (2013).
[43] S. Childress, and J. Strait, J. Phys. Conf. Ser. **408**, 012007 (2013).
[44] K. Abe *et al.* (T2K Collaboration), Phys. Rev. Lett. **112**, 181801 (2014).
[45] K. Abe *et al.* (T2K Collaboration), Phys. Rev. D **91**, 072010 (2015).
[46] D. Casper, Nucl. Phys. B, Proc. Suppl. **112**, 161 (2002).
[47] M. Honda, Phys. Rev. D **83**, 123001 (2011).
[48] T. Thakore, A. Ghosh, S. Choubey, and A. Dighe, J. High Energy Phys. 05 (2013) 058.
[49] M. M. Devi, T. Thakore, S. K. Agarwalla, and A. Dighe, J. High Energy Phys. 10 (2014) 189.
[50] D. Kaur, Z. A. Dar, S. Kumar, and M. Naimuddin, Phys. Rev. D **95**, 093005 (2017).
[51] A. Chatterjee, K. K. Meghna, R. Kanishka, T. Thakore, V. Bhatnagar, R. Gandhi, D. Indumathi, N. K. Mondal, and N. Sinha, J. Instrum. **9**, P07001 (2014).
[52] M. M. Devi, A. Ghosh, D. Kaur, S. M. Lakshmi, S. Choubey, A. Dighe, D. Indumathi, S. Kumar, M. V. N. Murthy, and M. Naimuddin, J. Instrum. **8**, P11003 (2013).
[53] M. C. Gonzalez-Garcia and M. Maltoni, Phys. Rev. D **70**, 033010 (2004).
[54] P. Huber, M. Lindner, and W. Winter, Comput. Phys. Commun. **167**, 195 (2005).
[55] P. Huber, J. Kopp, M. Lindner, M. Rolinec, and W. Winter, Comput. Phys. Commun. **177**, 432 (2007).
[56] S. Prakash, S. K. Raut, and S. U. Sankar, Phys. Rev. D **86**, 033012 (2012).
[57] P. Huber, M. Lindner, T. Schwetz, and W. Winter, J. High Energy Phys. 11 (2009) 044.
[58] M. Fechner, Détermination des performances attendues sur la recherche de l'oscillation numu to nue dans l'expérience T2K depuis l'étude des données recueillies dans l'expérience K2K (2006), http://inspirehep.net/record/722857/files/file.pdf.
[59] A. Ghosh, T. Thakore, and S. Choubey, J. High Energy Phys. 04 (2013) 009.